Thermal behavior and entanglement in Pb-Pb and *p-p* collisions

X. Feal, C. Pajares, and R. A. Vazquez
Instituto Galego de Física de Altas Enerxías and Departamento de Física de Partículas, Universidade de Santiago de Compostela, 15782 Santiago, Spain

(Received 1 June 2018; revised manuscript received 22 October 2018; published 24 January 2019)

The thermalization of the particles produced in collisions of small objects can be achieved by quantum entanglement of the partons of the initial state as was analyzed recently in proton-proton collisions. We extend such study to Pb-Pb collisions and to different multiplicities of proton-proton collisions. We observe that, in all cases, the effective temperature is approximately proportional to the hard scale of the collision. We show that such a relation between the thermalization temperature and the hard scale can be explained as a consequence of the clustering of the color sources. The fluctuations of the number of parton states decrease with multiplicity in Pb-Pb collisions as long as the width of the transverse-momentum distribution decreases, contrary to the *p-p* case. We relate these fluctuations to the temperature fluctuations by means of a Langevin equation for the white stochastic noise. We show that the multiplicity parton distribution for events with at least one hard parton collision is a Γ distribution. We use this result to compute the entanglement entropy, showing that the leading term is the logarithm of the number of partons, meaning that the n microstates are equally probable and the entropy is maximal. There is another contribution related to the inverse of the normalized parton number fluctuation, which at very high energy changes the behavior from $\ln n$ to $\ln \sqrt{n}$.

DOI: 10.1103/PhysRevC.99.015205

I. INTRODUCTION

The presence of an exponential shape in the transverse-momentum distribution (TMD) of the produced particles in collisions of small objects together with the approximate thermal abundances of the hadron yields constitutes an indicative sign of thermalization. This thermalization, however, cannot be achieved under the usual mechanism, namely, final-state interactions in the form of several secondary collisions.

The emergence of this phenomenon has been recently studied [1–4], showing that thermalization can be obtained during the rapid quench induced by the collision due to the high degree of entanglement inside the partonic wave functions of the colliding protons. Thus, the effective temperature obtained from the TMD of the particles produced in the collision depends on the momentum transfer; that is, it constitutes an ultraviolet cutoff of the quantum modes resolved by the collision. In diffractive processes with a rapidity gap, the entire wave function of the proton is involved and no entanglement entropy arises. Consequently, we expect no thermal radiation as it has been observed.

In this article we further explore the relation between parton entanglement and thermalization by studying *p-p* and Pb-Pb collisions at different multiplicities. In the second case we expect an interplay between thermalization and final-state interactions leading to some differences with *p-p* collisions concerning the entanglement and thermalization.

We show that the TMDs of both collisions at different multiplicities can be fitted by the sum of an exponential plus a powerlike function, characterized by a thermal-like temperature, $T_{\rm th}$, and a temperature scale, $T_{\rm h}$, respectively. For any fixed multiplicity and in all collisions the relation $4T_{\rm th} \approx T_{\rm h}$ is satisfied. The power index n describing the hard spectrum behaves differently in *p-p* and Pb-Pb collisions, showing the different behavior of the transverse-momentum fluctuations. This behavior and the relation between $T_{\rm th}$ and $T_{\rm h}$ can be naturally explained in the clustering of color sources. The cluster-size distribution of the clusters of overlapping strings found in the collision coincides with the distribution of temperatures obtained as the solution of the Fokker-Planck equation associated with the linear Langevin equation for a white Gaussian noise. We also show that the multiplicity of parton distribution for events with at least a hard parton is the Γ distribution. We take advantage of this result to compute the entanglement entropy. The leading contribution comes from the logarithm of the number of partons n. In addition, there is another contribution related to the width of the parton multiplicity. This contribution means, asymptotically, that the entanglement entropy becomes the logarithm of $\sqrt{n}$, indicating that the number of effective microstates changes with energy from n to $\sqrt{n}$.

The organization of the article is as follows. In Sec. II we introduce the entanglement of the partonic state following Ref. [1] and we analyze the TMD of *p-p* and Pb-Pb collisions at different multiplicities. In Sec. III we discuss the obtained results, remarking on the similarities and differences

of p-p and Pb-Pb collisions in connection with thermalization and entanglement. We briefly discuss the clustering of color sources in connection with the TMD in Sec. IV, and in Sec. V we introduce the Langevin and Fokker-Planck equations to study the time temperature fluctuations. In Sec. VI, we study the conditional multiplicity distributions for events with at least a hard parton collision, and in Sec. VII we compute the entanglement entropy. Finally in Sec. VIII the conclusions are presented.

II. ENTANGLEMENT, THERMALIZATION, AND TRANSVERSE MOMENTUM DISTRIBUTIONS

A hard process with momentum transfer Q probes only the region of space H of transverse size $1/Q$. Let us denote by S the region of space complementary to H. The proton is described by the wave function,

$$|\Psi_{HS}\rangle = \sum_n \alpha_n |\Psi_n^H\rangle |\Psi_n^S\rangle, \tag{1}$$

of a suitably chosen orthonormal set of states $|\Psi_n^H\rangle$ and $|\Psi_n^S\rangle$ localized in the domains H and S. In the parton model this full orthonormal set of states is given by the Fock states with different numbers n of partons. The state (1) cannot be separated into a product, $|\varphi^H\rangle \otimes |\varphi^S\rangle$, and therefore $|\Psi_{HS}\rangle$ is entangled. The density matrix of the mixed state probed in region H is

$$\begin{aligned}\rho_H &= \mathrm{Tr}_S\, \rho_{SH} \\ &= \sum_n \langle \Psi_n^S | \Psi_{HS}\rangle \langle \Psi_{HS} | \Psi_n^S\rangle \\ &= \sum_n |\alpha_n|^2 |\Psi_n^H\rangle \langle \Psi_n^H|,\end{aligned} \tag{2}$$

where $|\alpha_n|^2 = p_n$ is the probability of having a state with n partons, independently of whether their interaction is hard or soft. The von Neumann entropy of this state is given by

$$S = -\sum_n p_n \ln p_n. \tag{3}$$

We can consider that a high-momentum partonic configuration of the proton when the collision takes place undergoes a rapid quench due to the QCD interaction. The onset τ of this hard interaction is given by the hardness scale Q, $\tau \sim 1/Q$. Because τ is small the quench creates a highly excited multiparticle state. The produced particles have a thermal-like exponential spectrum with an effective temperature, $T \approx (2\pi\tau)^{-1} \approx Q/2\pi$. Thus, the thermal spectrum can be originated due to the event horizon formed by the acceleration of the color field [5–9]. On the other hand, the comparison with CERN Large Hadron Collider (LHC) data on hadron multiplicity distributions [2] indicates that the produced Boltzmann entropy is close to the entanglement entropy of Eq. (3).

In Ref. [1], the thermal component of charged-hadron transverse-momentum distribution in p-p collisions at $\sqrt{s} =$ 13 TeV is parametrized as [10–12]

$$\frac{1}{N_{\rm ev}} \frac{1}{2\pi p_t} \frac{d^2N_{\rm ev}}{d\eta dp_t} = A_{\rm th} \exp(-m_t/T_{\rm th}), \tag{4}$$

where $T_{\rm th}$ is the effective temperature and $m_t = \sqrt{m^2 + p_t^2}$ is the transverse mass. The hard scattering, meanwhile, is parametrized as

$$\frac{1}{N_{\rm ev}} \frac{1}{2\pi p_t} \frac{d^2N_{\rm ev}}{d\eta dp_t} = A_{\rm h} \frac{1}{\left(1 + \frac{m_t^2}{nT_{\rm h}^2}\right)^n}, \tag{5}$$

where the temperature $T_{\rm h}$ and the index n are parameters determined from the fit to the experimental data. The value $T_{\rm th} = 0.17$ GeV was found [1], agreeing with the one expected from the extrapolation of the relation

$$T_{\rm th} = 0.098 \left(\sqrt{\frac{s}{s_0}}\right)^{0.06} \ (\mathrm{GeV}), \tag{6}$$

obtained at lower energies. Similarly the hard scale $T_{\rm h}$ is given by the relation

$$T_{\rm h} = 0.409 \left(\sqrt{\frac{s}{s_0}}\right)^{0.06} \ (\mathrm{GeV}). \tag{7}$$

At $\sqrt{s} = 13$ TeV, the values found for the hard scale are $T_{\rm h} =$ 0.72 GeV and $n = 3.1$. We notice that from Eqs. (6) and (7) one finds

$$\frac{T_{\rm h}}{T_{\rm th}} \approx 4.2, \tag{8}$$

independently of the energy. The ratios of the particular values obtained in the fit [1] are close to these values.

To study the dependence on the multiplicity of $T_{\rm th}$ and $T_{\rm h}$ we have used the transverse-momentum distribution of K_S^0 produced in p-p collisions at $\sqrt{s} = 7$ TeV in the range up to $p_t \leqslant 10$ GeV/c [13]. We use K_S^0 instead of π or charged particles because we have not found published data covering a broad range of soft and hard regions at different multiplicities. In Figs. 1–3, we show the fit and the results for $T_{\rm h}$ and

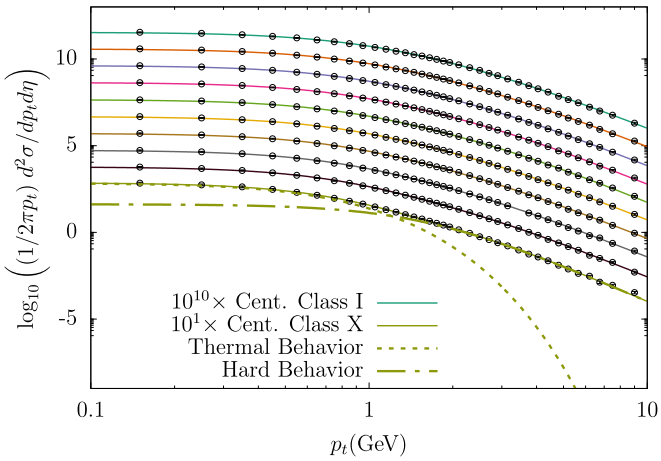

FIG. 1. Normalized differential K_S^0 production in p-p collisions at $\sqrt{s_{NN}} = 7$ TeV as a function of transverse momentum for different classes of centralities. Centrality classes from I to X, in decreasing magnitude, correspond to charged-particle productions of $dN_{\rm ch}/d\eta = 21.3$, 16.5, 13.5, 11.5, 10.1, 8.45, 6.72, 5.40, 3.90, and 2.26. The thermal and hard components of the lowest centrality fit are shown by short dashed and long dashed lines, respectively.

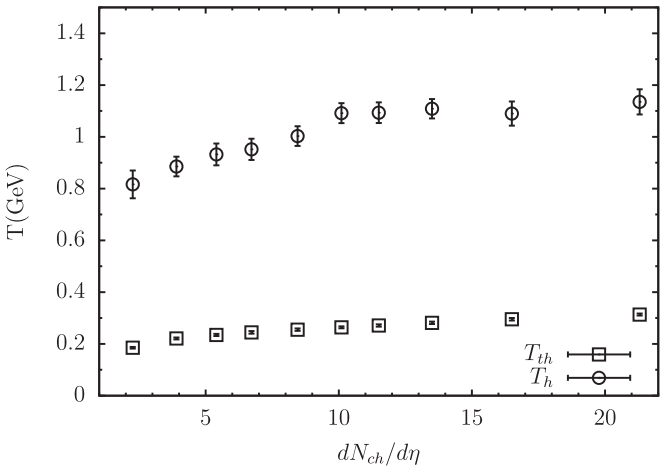

FIG. 2. $T_{\rm th}$ and $T_{\rm h}$ as a function of centrality for K^0_S production in p-p collisions at $\sqrt{s_{NN}} = 7$ TeV.

$T_{\rm th}$, respectively, as a function of $dN_{\rm ch}/d\eta$. We observe an increase of $T_{\rm h}$ and $T_{\rm th}$. The values of $T_{\rm th}$ and $T_{\rm h}$ are in the ranges 0.18–0.28 and 0.8–1.15, respectively. In Fig. 3 the scaled curve $4T_{\rm th}$ is shown compared to $T_{\rm h}$. We observe that the scaled $4T_{\rm th}$ curve lies on the obtained $T_{\rm h}$ values; therefore the relation between $T_{\rm th}$ and $T_{\rm h}$ (8) remains approximately valid not only for different energies but also for different centralities, pointing to some physical reason. The obtained values for $T_{\rm th}$ and $T_{\rm h}$ are slightly higher than the values of $T_{\rm th} = 0.17$ GeV and $T_{\rm h} = 0.74$ GeV of Ref. [1] due to the different sets of data, because in this analysis K^0_S is used instead of charged particles.

We have extended the study to Pb-Pb collisions at different multiplicities by fitting the ALICE Collaboration TMD data for charged particles [14] at $\sqrt{s} = 2.76$ TeV. In Figs. 4–6, we show the fit and the values obtained for $T_{\rm th}$ and $T_{\rm h}$ as a function of the multiplicity. $T_{\rm th}$ also increases with multiplicity and $T_{\rm h}$ follows the same relation $T_{\rm h} \approx 4T_{\rm th}$ observed at p-p collisions.

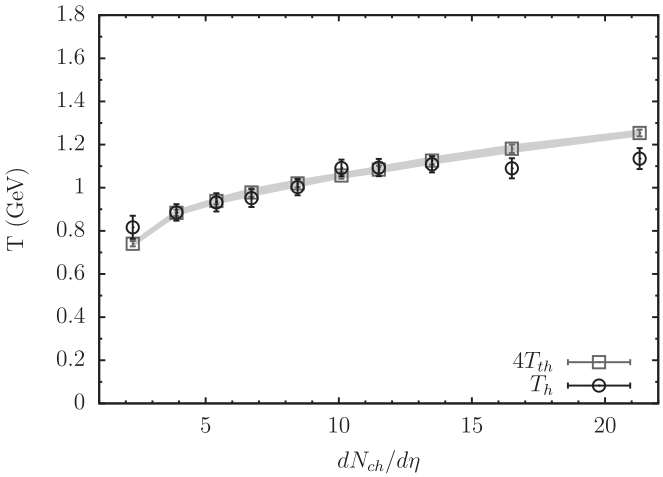

FIG. 3. $T_{\rm h}$ and $4T_{\rm th}$ as a function of centrality for K^0_S production in p-p collisions at $\sqrt{s_{NN}} = 7$ TeV.

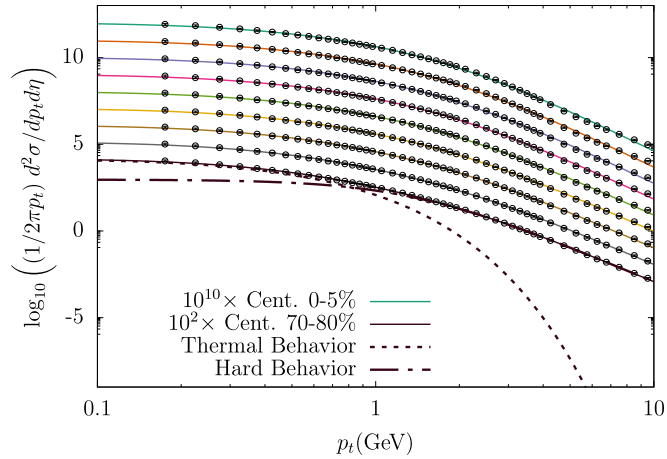

FIG. 4. Normalized differential charged-particle production in Pb-Pb collisions at $\sqrt{s_{NN}} = 2.76$ TeV, as a function of transverse momentum for different classes of centralities. Centrality classes from 0%–5% to 70%–80%, in decreasing magnitude, correspond to charged-particle productions of $dN_{\rm ch}/d\eta = 1600$, 1290, 960, 650, 425, 260, 145, 75, and 30. The thermal and hard components of the lowest centrality fit are shown by short-dashed and long-dashed lines, respectively.

In Fig. 7 we show the results of the fit for the power index n in p-p and Pb-Pb collisions as a function of the charged-particle production. n decreases with multiplicity for p-p collisions and, on the contrary, increases for Pb-Pb collisions. For p-p collisions at $\sqrt{s} = 13$ TeV the value obtained for the case of charged particles is $n = 3.1$, slightly smaller than the value shown in Fig. 7. The values of n are larger for Pb-Pb collisions than for p-p collisions as expected due to the jet quenching and corresponding to high-p_t particle suppression.

III. DISCUSSION

Our results for p-p collisions show that for each multiplicity the effective thermal temperature obtained from the TMD

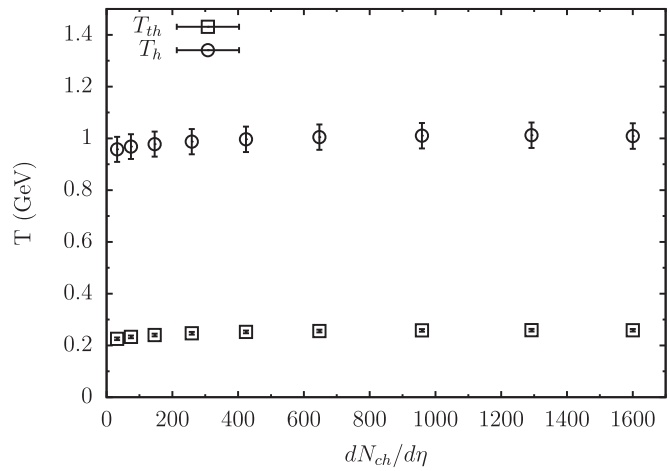

FIG. 5. Variation of $T_{\rm th}$ and $T_{\rm h}$ with centrality for charged-particle production in Pb-Pb collisions at $\sqrt{s} = 2.76$ TeV.

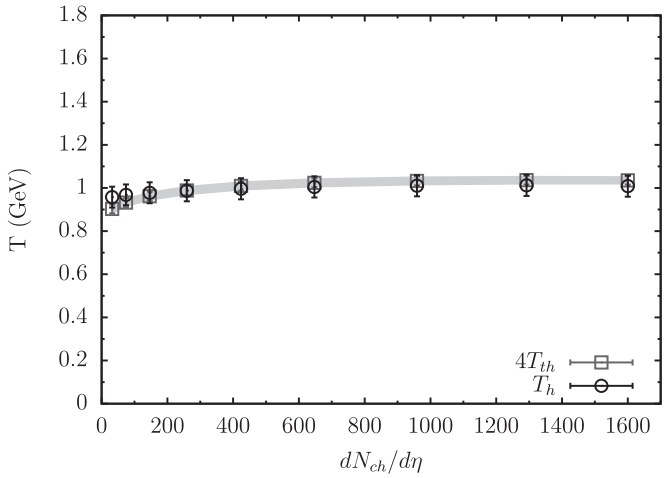

FIG. 6. $T_{\rm h}$ and $4T_{\rm th}$ as a function of centrality for charged-particle production in Pb-Pb collisions at $\sqrt{s} = 2.76$ TeV.

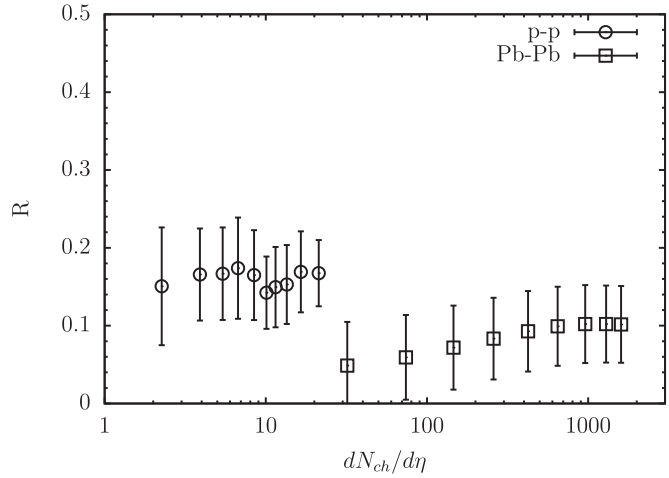

FIG. 8. R, the ratio of the hard component to the total component as a function of $dN_{\rm ch}/d\eta$, for K^0_S production in p-p at $\sqrt{s} = 7$ TeV and for charged-particle production in Pb-Pb collisions at $\sqrt{s_{NN}} = 2.76$ TeV.

of the produced particles can be viewed as a rapid quench of the entangled partonic state. The behavior of $T_{\rm th}$ and $T_{\rm h}$ as a function of the multiplicity is very similar, holding the relation $T_{\rm h} \approx 4T_{\rm th}$ for all the studied multiplicities. This fact adds evidence to the cases studied in Ref. [1]. It is remarkable that the same relation holds for Pb-Pb collisions, realizing the different values of $T_{\rm th}$ and $T_{\rm h}$ compared with the those in the p-p case. The increase of $T_{\rm th}$ with multiplicity in p-p collisions is larger than that in the Pb-Pb case as was expected, as long as $T_{\rm th}$ was nothing but $\langle p_t \rangle$, and experimentally the LHC data [14] have shown an increase with multiplicity in p-p collisions that is larger than that in Pb-Pb collisions.

Equations (4) and (5) can be obtained in the framework of clustering of color sources [15–17] as we show in Sec. IV. In this approach the cluster-size distribution is a Γ distribution [18–21] that coincides with the stationary solution of the Fokker-Planck equation derived from the Langevin equation corresponding to a white noise [22,23]. In this way the fluctuations in the cluster size are related to the temperature fluctuations.

The ratio R of the integral under the power-law curve (hard component) and the integral over the total (hard + thermal components),

$$R = \frac{H}{H+S}, \tag{9}$$

is plotted in Fig. 8 for different multiplicities for p-p and Pb-Pb collisions. The value found at $\sqrt{s} = 13$ TeV in Ref. [1] was $R \approx 0.16$, in agreement with the ratio calculated in inelastic proton-proton collisions at $\sqrt{s} = 23$, 31, 45, and 53 GeV. Our results for p-p collisions at $\sqrt{s} = 7$ TeV for different multiplicities are close to the mentioned value. In the case of Pb-Pb we have found a smaller value. This smallness is consistent with the behavior found in Ref. [24] based on saturation momentum and geometrical scaling.

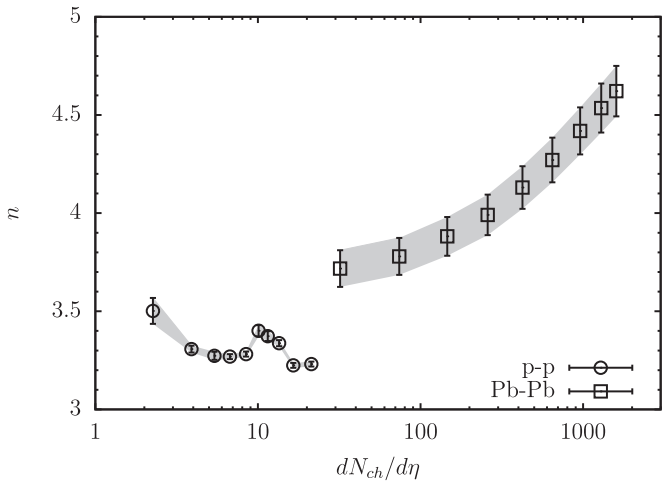

FIG. 7. Power index n of the hard component as a function of $dN_{\rm ch}/d\eta$ for K^0_S production in p-p at $\sqrt{s} = 7$ TeV and for charged-particle production in Pb-Pb collisions at $\sqrt{s_{NN}} = 2.76$ TeV.

IV. CLUSTERING OF COLOR SOURCES

Multiparticle production is currently described in terms of color sources (strings) stretched between the projectile and the target. These strings decay by the Schwinger q-$\bar{q}$ production and subsequently hadronize to produce the observed hadrons. The color in the strings is confined in a small area in the transverse space of the order of 0.2 fm. With increasing energy and/or atomic number of the colliding objects, the number of color sources grows, and they start to overlap, forming clusters. A cluster of n color sources behaves as a single string with an energy momentum that corresponds to the sum of the energy momentum of the overlapping strings and with a higher color field, corresponding to the vectorial sum of the color charges of each individual string. The resulting color field covers the area S_n of the cluster. Thus $\vec{Q}_n^2 = (\sum_1^n \vec{Q}_i)^2$, and given that the individual string colors can be arbitrarily oriented in color space, the average $\vec{Q}_i \cdot \vec{Q}_j$ is zero, so $\vec{Q}_n^2 = n\vec{Q}_1^2$. As Q_n depends also on the area, we have

$Q_n = \sqrt{nS_n/S_1}Q_1$, where S_1 is the area of the individual string. The mean multiplicity and the mean transverse momentum are proportional to the color charge and to the color field, respectively,

$$\mu_n = \sqrt{\frac{nS_n}{S_1}}\mu_1, \quad \langle p_t^2\rangle_n = \sqrt{\frac{nS_1}{S_n}}\langle p_t^2\rangle_1, \tag{10}$$

which in the limit of high density, $\xi = N_s S_1/S$, becomes

$$\mu_n = N_s F(\xi)\mu_1, \quad \langle p_t^2\rangle_n = \frac{1}{F(\xi)}\langle p_t^2\rangle_1, \tag{11}$$

where N_s is the number of color sources and $F(\xi)$ is a universal factor,

$$F(\xi) = \sqrt{\frac{1-e^{-\xi}}{\xi}}. \tag{12}$$

The factor $1-e^{-\xi}$ is the fraction of the total collision area covered by color sources at density ξ (a homogeneous profile for the collision area is assumed). $F(\xi)$ goes to 1 at low densities and goes to 0 at high ξ. The transverse-momentum distribution $f(p_t)$ is obtained from the Schwinger's distribution, $\exp(-p_t^2 x)$, weighted by the cluster-size distribution $W(x)$, where x is the inverse of $\langle p_t^2\rangle_n$:

$$f(p_t) = \int dx W(x)\exp\left(-p_t^2 x\right). \tag{13}$$

The weight function is the Γ distribution because the process of increasing the centrality or energy of the collision can be regarded as a transformation of the color field located in the sites of the surface area, implying a transformation of the cluster-size distribution of the type

$$W(x') \to \frac{x' W(x')}{\langle x'\rangle} \to \cdots \frac{x'^k W(x')}{\langle x'^k\rangle} \to \cdots. \tag{14}$$

This renormalization group type of transformation was studied a long time ago in probability theory, and it was shown that the only stable distributions under such transformations are generalized Γ distributions. We take the simplest case, namely, the Γ distribution

$$W(x) = \frac{\gamma}{\Gamma(n)}(\gamma x)^{n-1}\exp(-\gamma x), \tag{15}$$

with

$$\gamma = \frac{n}{\langle x\rangle} \tag{16}$$

and

$$\frac{1}{n} = \frac{\langle x^2\rangle - \langle x\rangle^2}{\langle x\rangle^2}. \tag{17}$$

Introducing Eq. (15) into Eq. (13) we obtain the distribution [18]

$$f(p_t) = \frac{1}{\left(1+p_t^2/\gamma\right)^n} = \frac{1}{\left(1+\frac{F(\xi)p_t^2}{n\langle p_t^2\rangle_1}\right)^n}, \tag{18}$$

which takes the form of the parametrization used in Eq. (5) with

$$T_{\rm h}^2 = \frac{\langle p_t^2\rangle_1}{F(\xi)}, \tag{19}$$

which grows with the density ξ and thus with the energy and centrality as is observed in the analysis of p-p and Pb-Pb collisions. In the last case, if the fits include larger p_t values a flattening of the dependence of $T_{\rm h}$ with multiplicity due to jet quenching effects is observed. At low p_t, Eq. (18) behaves as

$$f(p_t) \approx \exp\left(-p_t^2 F(\xi)/\langle p_t^2\rangle_1\right), \tag{20}$$

independently of n. In this low-p_t regime, there are other effects, like fluctuations of the color field, that should be taken into account. In fact, assuming that such fluctuations are Gaussian, we have [6–8]

$$P(T_{\rm h}) = \sqrt{\frac{2}{\pi\sigma^2}}\exp\left(-\frac{T_{\rm h}^2}{2\sigma^2}\right), \tag{21}$$

hence we obtain the thermal distribution

$$f_{\rm th}(p_t) = \int_0^\infty dT_{\rm h} P(T_{\rm h})\exp\left(-\frac{p_t^2}{T_{\rm h}^2}\right) = \exp\left(-\frac{p_t}{\sigma/\sqrt{2}}\right). \tag{22}$$

In other words, the thermal temperature is proportional to the fluctuations of the hard temperature, which are proportional to the hard temperature. The exact relation between the hard and thermal scales, however, must account for the effect of the fluctuations in the hard part of the distribution in the width of the found soft distribution.

We notice that according to Eq. (18) the power index n is related to the inverse of the width of the distribution and a different behavior with multiplicity is obtained for p-p and Pb-Pb collisions. This fact is a consequence of the clustering of the color sources. At low density of sources, there are only a few clusters of overlapping strings and thus the only temperature fluctuations come from inside the individual strings. As the number of clusters with different numbers of color sources increases, the fluctuations also increase and correspondingly n decreases. If the color density increases further, the clusters of different colors start to overlap in such a way that the number of clusters with different numbers of color sources decreases and thus the fluctuations decrease and n increases. The change of behavior that can be observed in Fig. 7 is related to the critical percolation point. Notice that n is decreasing with multiplicity in p-p collisions, but we expect that above a given multiplicity n should start to grow in the same way as in Pb-Pb collisions.

V. THERMAL BEHAVIOR AND NON-GAUSSIAN DISTRIBUTION

The Gibbs distribution in energy, $\exp(-E/T)$, which is Gaussian in the momenta of free massive particles, $\exp(-\boldsymbol{p}^2/2mT)$, is considered as the generalized case for thermal equilibrium of noncorrelated or short-range correlated systems. A microdynamical explanation for the Maxwell-Boltzmann statistics is given by the Langevin equation, describing a particle moving under the influence of a

deterministic damping force and a stochastic drive, which accelerates the particle in a short time, changing the momenta randomly and uncorrelated. The stationary solution of this stochastic equation follows the Gaussian distribution. Because the harmonic oscillator is just the extension of this free-motion Langevin equation into the phase space, this picture is also accepted for free quantum systems.

It could be thought that any non-Gaussian distribution may only come from nonthermalized systems, in particular, the obtained power-tail distribution or the Γ distribution, which gives rise to the power-tail distribution in the clustering of color sources model. However, it has been shown [23] that this is not the case, and by treating the deterministic damping constant in the Langevin equation also stochastically then the distribution is in general non-Gaussian. In particular for the case of a multiplicative white noise it is a Γ distribution [22].

Let us consider the Langevin equation of a variable σ for a stochastic process [22]:

$$\frac{d\sigma}{dt} + \left(\frac{1}{\tau} + \xi(t)\right)\sigma = \phi. \tag{23}$$

The stochastic process is defined by the white Gaussian noise $\xi(t)$ with the mean $\langle\xi(t)\rangle$ and the correlator $\langle\xi(t)\xi(t+\Delta t)\rangle$ given, respectively, by

$$\langle\xi(t)\rangle = 0, \quad \langle\xi(t)\xi(t+\Delta t)\rangle = 2D\delta(\Delta t), \tag{24}$$

where τ and D define, respectively, the mean time for changes of the variable σ and its variance by the following conditions:

$$\langle\sigma(t)\rangle = \sigma(0)\exp(-t/\tau), \quad \langle\sigma^2(\infty)\rangle = \frac{\tau D}{2}. \tag{25}$$

From Eq. (23) a Fokker-Planck equation can be obtained, following the procedure of Ref. [23], for the probability distribution $f(\sigma, t)$ of having the value $\sigma(t+\delta t)$, provided the value at time t is $\sigma(t)$, and the noise $1/\tau + \xi$, namely [22],

$$\frac{\partial f(\sigma)}{\partial t} = -\frac{\partial}{\partial\sigma}K_1(\sigma)f(\sigma) + \frac{1}{2}\frac{\partial^2}{\partial\sigma^2}K_2(\sigma)f(\sigma), \tag{26}$$

with

$$K_1(\sigma) = -\frac{1}{\tau}\sigma + \phi, \quad K_2(\sigma) = 2D\sigma^2. \tag{27}$$

The stationary solution of Eq. (26) is

$$f(\sigma) \sim \frac{1}{K_2(\sigma)}\exp\left(2\int ds\frac{K_1(s)}{K_2(s)}\right), \tag{28}$$

which once normalized and by using Eq. (27) becomes the Γ distribution

$$f(\sigma) = \frac{1}{\Gamma(n)}\frac{\mu^n}{\sigma^{1+n}}\exp\left(-\frac{\mu}{\sigma}\right), \tag{29}$$

with

$$\mu = \frac{\phi}{D}, \quad n = 1 + \frac{1}{\tau D}. \tag{30}$$

We observe that by taking the variable as $\sigma = T_{\rm h}^2 = 1/x$ the Γ distribution in Eq. (29) is nothing but the Γ distribution as defined in Eq. (15) with $\mu = \gamma = n/\langle T_{\rm h}\rangle^2$. From Eq. (30) we have

$$\langle T_{\rm h}^2\rangle = \tau\phi, \tag{31}$$

meaning that the higher $T_{\rm h}^2$, the scale of hard interactions, is the higher $\tau$is ; thus T_h and $T_{\rm th}$ evolve slowly.

VI. CONDITIONAL PROBABILITY FOR A HARD COLLISION

Let us consider the probability p_n of having n partons in a given collision. It has been shown [25–29] that the conditional probability p_n^c of having n partons and at least one giving rise to a hard collision is

$$p_n^c = \frac{n}{\langle n\rangle}p_n. \tag{32}$$

This equation has been obtained not only for hard events but also for events of a type, denoted by c, in which for a result to be considered of the type c it is enough to have a single c event in at least one of the elementary collisions. Examples of this kind are events without a rapidity gap (nondiffractive events), hard events, annihilation events in $\bar{p}$-p collisions, events with at least one jet and $W^{\pm}$ and Z^0 events. Let $N(n)$ be the number of events with n being the number of elementary collisions observed in a hadronic or nuclear collision, we then have

$$N(n) \equiv \sum_{i=0}^{n}\binom{n}{i}\alpha_c^i(1-\alpha_c)^{n-i}N(n), \tag{33}$$

where α_c is the probability of having an event c in an elementary collision ($0 < \alpha_c < 1$). If α_c is small, Eq. (33) becomes

$$N(n) = \alpha_c nN(n) + (1-\alpha_c n)N(n), \tag{34}$$

where from the definition of a type c event the first term of Eq. (34) is the number of events $N_c(n)$ where a c occurs:

$$N_c(n) = \alpha_c nN(n). \tag{35}$$

If N is the total number of events, we have

$$\sum_n N(n) = N, \quad \sum_n n^k N(n) \equiv \langle n^k\rangle N, \tag{36}$$

and for the total number of events with c occurring, we have

$$\sum_n \alpha_c nN(n) = \alpha_c\langle n\rangle N. \tag{37}$$

This implies the following for the probability distribution of having a c event in n collisions:

$$p_c(n) = \frac{\alpha_c nN(n)}{\alpha_c\langle n\rangle N} = \frac{n}{\langle n\rangle}p(n), \tag{38}$$

which is of the form of Eq. (32). In this equation, n is the number of elementary collisions (parton-parton or nucleus-nucleus, depending on the case studied), but Eq. (38) has been applied to the multiplicity particle probability distributions, $p(n)$ being the minimum bias multiplicity distribution. Indeed, Eq. (32) was checked in the case of production of $W^{\pm}$ and Z^0 with data of the CDF Collaboration at Fermilab [26], in the case of the production of jet events with data of the UA1 Collaboration at CERN Super Proton Synchrotron [26], in the case of the production of Drell-Yan pairs in S-U collisions

with data of the NA38 Collaboration [27], and in the case of annihilation in $\bar{p}p$ collisions [26]. In all cases a good agreement with the experimental data was obtained. Notice that in Eq. (32) the right-hand side is independent of c and only its shape is determined by the requirement of being of type c. In terms of cross sections, the c events are self-shadowed, and their cross sections can be written as a function of only the elementary cross sections of a c event [30,31].

This selection procedure of the events satisfying certain c criteria can be repeatedly applied for subsequent c conditions. For instance, from these events with at least one particle with transverse momentum larger than $p_{t,1}$ one can further select events with at least one particle with transverse momentum larger than $p_{t,2}$ and $p_{t,2} > p_{t,1}$, and so on (there are cases in which this multiple selection procedure cannot be applied more than once, like nondiffractive or annihilation events). The corresponding probability distributions to the repeated selection satisfy

$$p(n) \to \frac{n}{\langle n\rangle}p(n) \to \frac{n^2}{\langle n^2\rangle}p(n) \to \cdots \frac{n^k}{\langle n^k\rangle}p(n). \tag{39}$$

Notice that

$$\langle n\rangle_c = \frac{\langle n^2\rangle}{\langle n\rangle} \tag{40}$$

and

$$\langle n\rangle_c - \langle n\rangle = \frac{\langle n^2\rangle - \langle n\rangle^2}{\langle n\rangle} \geqslant 0. \tag{41}$$

As we say in Sec. IV, transformations of the kind of Eq. (39) were studied a long time ago by Jona-Lasinio [32] in connection with the renormalization group in probability theory, showing that the only stable probability distributions under such transformations are the generalized Γ distributions. The simplest one is the Γ distribution. This transformation has also been studied in connection with the self-similarity condition and the KNO scaling [29]:

$$\langle n\rangle p_n = \psi\left(\frac{n}{\langle n\rangle}\right) = \psi(z). \tag{42}$$

For the Γ distribution

$$\psi(z) = \frac{\beta^k}{\Gamma(k)}z^{k-1}e^{-\beta z}, \quad k > 1, \tag{43}$$

we have the normalization conditions

$$1 \equiv \sum_n p_n = \sum_n \frac{1}{\langle n\rangle}\psi\left(\frac{n}{\langle n\rangle}\right) = \int dz\psi(z) = 1 \tag{44}$$

and

$$1 \equiv \sum_n \frac{n}{\langle n\rangle}p_n = \int dzz\psi(z), \tag{45}$$

which forces $\beta = k$. The parameter k is related to the normalized width:

$$\frac{1}{k} = \frac{\langle z^2\rangle - \langle z\rangle^2}{\langle z\rangle^2}. \tag{46}$$

We use the Γ distribution in our evaluations of the entanglement entropy.

The origin of the nonextensive thermodynamics related to Eq. (5) could be the fractal structure of the thermodynamical system. In Ref. [33] it is shown that such systems present temperature fluctuations following a γ distribution. The repetitive fractal structure has to do with the scale transformations represented by Eq. (39).

In terms of the reduced matrix density (2), the transformation induced by the repeated selection $p_{t,1} < p_{t,2} < \cdots < p_{t,j}$ translates into a sum over each time of a larger region of soft partons, modifying the probability $p_n = |\alpha_n|^2$ in the way prescribed by the chain in Eq. (39).

VII. ENTANGLEMENT ENTROPY

We use Eq. (43) to evaluate the entanglement entropy. The von Neumann entropy for minimum bias events is

$$\begin{aligned} S &= -\sum_n p_n \ln p_n \\ &= -\sum_n \frac{1}{\langle n\rangle}\psi\left(\frac{n}{\langle n\rangle}\right)\ln\left[\frac{1}{\langle n\rangle}\psi\left(\frac{n}{\langle n\rangle}\right)\right] \\ &= \ln\langle n\rangle - \int_0^\infty dz\psi(z)\ln[\psi(z)], \end{aligned} \tag{47}$$

and the von Neumann entropy for type c events, containing at least one hard collision, is

$$\begin{aligned} S^c &= -\sum_n p_n^c \ln p_n^c = -\sum_n \frac{np_n}{\langle n\rangle}\ln\left(\frac{np_n}{\langle n\rangle}\right) \\ &= -\sum_n \frac{n}{\langle n\rangle^2}\psi(z)\ln\left(\frac{n\psi(z)}{\langle n\rangle^2}\right) \\ &= -\int_0^\infty dzz\psi(z)\ln\left(\frac{z\psi(z)}{\langle n\rangle}\right) \\ &= \ln\langle n\rangle - \int_0^\infty dzz\psi(z)\ln[z\psi(z)]. \end{aligned} \tag{48}$$

Taking for $\psi(z)$ the Γ distribution, we obtain

$$\begin{aligned} S &= \ln\langle n\rangle - \ln k + k + \ln\Gamma(k) + \frac{1-k}{\Gamma(k)}\partial_k\Gamma(k) \\ &\simeq \ln\langle n\rangle + \frac{1}{2}\left[\frac{k-1}{k} + \ln\left(\frac{2\pi}{k}\right)\right] \\ &\to \ln\frac{\langle n\rangle}{\sqrt{k}} = \ln\langle n\rangle^{1/2} \end{aligned} \tag{49}$$

and

$$\begin{aligned} S^c &= \ln\langle n\rangle + k + \ln\Gamma(k) - \frac{k}{\Gamma(k)}\partial_k\Gamma(k) \\ &\simeq \ln\langle n\rangle + \frac{1}{2}\left[1 + \ln\left(\frac{2\pi}{k}\right)\right] \\ &\to \ln\frac{\langle n\rangle}{\sqrt{k}} = \ln\langle n\rangle^{1/2}, \end{aligned} \tag{50}$$

where the last equality of the above relations holds for large k and $\Gamma(k)$ is the Γ function. We observe that the leading term $\ln\langle n\rangle$, given that $\langle n\rangle \simeq s^\Delta$, is similar to the one obtained using

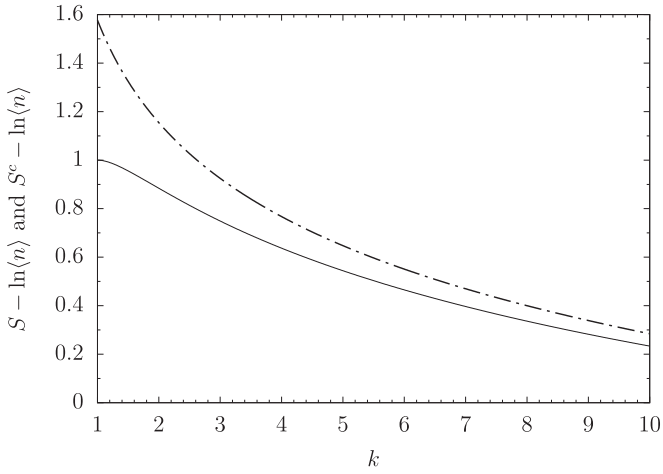

FIG. 9. Entanglement entropy $S - \ln\langle n\rangle$ (49) of the minimum bias distribution $p(n)$ (42) (solid line) and entanglement entropy $S^c - \ln\langle n\rangle$ (50) of the type c event distribution $p_c(n)$ (38) (dot-dashed line).

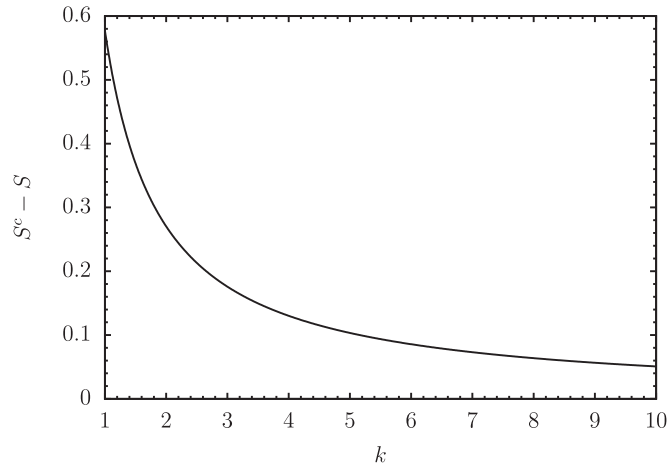

FIG. 10. Entanglement entropy difference $S^c - S$ of Eqs. (49) and (50) for the minimum bias distribution $p(n)$ (42) and for the type c event distribution $p_c(n)$ (38).

the Balitsky-Kovchegov equation. The difference between both entropies reads

$$S^c - S = \ln k - \frac{1}{\Gamma(k)}\partial_k\Gamma(k) \simeq \frac{1}{2k}, \tag{51}$$

In Fig. 9 $S - \ln\langle n\rangle$ and $S^c - \ln\langle n\rangle$ are shown as a function of k. As $k > 1$, S and S^c decrease with k and at larger values S^c approaches S. As $k > 1$, $S - \ln\langle n\rangle$ and $S^c - \ln\langle n\rangle$ are decreasing functions of k in all the allowed domain of k. These functions, according to Eqs. (49) and (50), become negative at very high k. The leading term of S and S^c is $\ln\langle n\rangle$, meaning that the n partons, i.e., the n microstates of the system, are equally probable, and thus the entropy is maximal. In addition to this contribution, there is one that depends only on k, i.e., the inverse of the normalized fluctuations on the number of partons, Eq. (50). This contribution is a positive decreasing function of k in a very broad range, becoming negative at very high k. In the infinite limit, the Γ distribution becomes the normal or Gaussian distribution, and both S and S^c behave like $\ln(n/\sqrt{k}) = \ln(n^{1/2})$. This result means that the number of microstates is not n anymore but rather $\sqrt{n}$. A saturation effect occurs and the growth of microstates is suppressed as the collision energy or the centrality increases. This saturation is explained in models like the color glass condensate (CGC) or the clustering of color sources. In this last model, the number of independent color sources or strings, n, formed from the initial partons of the colliding objects, is reduced at high energies because the number of effective independent color sources is proportional to $\sqrt{n}$ in such a way that Eq. (50), involving logarithms, is satisfied [34]. In the limit of high energy in the glasma picture of the CGC, the number of color flux tubes is also $\sqrt{n}$.

It could be thought that because $\langle n\rangle_c \geqslant \langle n\rangle$ the leading term of the entanglement entropy S^c is larger than the corresponding S. Indeed, instead of Eq. (48) we could have written

$$S^c = \ln\langle n\rangle_c - \int dz\psi_c(z)\ln[\psi_c(z)], \tag{52}$$

with

$$\psi_c(z) \equiv \frac{1}{\langle n\rangle_c}p_n^c = \frac{1}{\langle n\rangle_c}\frac{n}{\langle n\rangle}p_n = \frac{1}{\langle n\rangle_c}\psi(z). \tag{53}$$

From Eqs. (46) and (40) we can write

$$\ln\langle n\rangle_c = \ln\langle n\rangle + \ln\left(1 + \frac{1}{k}\right), \tag{54}$$

so asymptotically as $k \to \infty$, $\langle n_c\rangle = \langle n\rangle$.

The differences between S and S^c are small and asymptotically tend to zero as is shown in Fig. 10.

The dependence of $S - \ln\langle n\rangle$ or $S^c - \ln\langle n\rangle$ on the energy or on the impact parameter (centrality) is very interesting in the clustering of color sources approach due to the previously described dependence of k on the string density ξ. At low density, k decreases up to a critical string density, ξ_c. Above this critical density, $\xi > \xi_c$, k increases. In this way, both $S - \ln\langle n\rangle$ and $S^c - \ln\langle n\rangle$ increase with ξ up to the critical density ξ_c and decrease for larger ξ. This decrease of $S - \ln\langle n\rangle$ or $S^c - \ln\langle n\rangle$ with energy or centrality is small compared with the growth of $\ln\langle n\rangle$ in such a way that S and S^c are always growing. The exact value of k, which corresponds to the ξ_c marking the turnover, depends on the observed rapidity range, the p_t acceptance, and the profile functions of the projectile and the target. We know from the data that k decreases with energy and centrality in p-p collisions and it increases for Au-Au and Pb-Pb collisions. The turnover of k could be at very high multiplicity in p-p collisions at $\sqrt{s} = 13$ TeV. Notice that S or S^c does not present a maximum at $\xi = \xi_c$ but rather a change in the dependence of S or S^c on ξ.

VIII. CONCLUSIONS

The analysis of the dependence on the multiplicity of the LHC p-p and Pb-Pb data confirms the picture of thermalization induced by quantum entanglement. In all the analyzed data, the effective thermalization temperature obtained from the data is proportional to the hard scale of the collision T_h

given by the average transverse momentum. The coefficient of proportionality is universal, independent of the considered collision, even though $T_{\rm th}$ and $T_{\rm h}$ are different in each collision type. Thermal and hard temperatures increase with multiplicity in both collision scenarios, and this rise reproduces the known correlation of $\langle p_t \rangle$ and $dN_{ch}/d\eta$ for p-p and Pb-Pb collisions. In the framework of clustering of color sources the proportionality between $T_{\rm th}$ and $T_{\rm h}$ is understood, being $T_{\rm th}$ proportional to the fluctuations of $T_{\rm h}$. The n parameter of the hard distribution decreases with multiplicity for p-p collisions and increases for Pb-Pb collisions. This fact means that the normalized transverse-momentum fluctuations behave quite different with multiplicity in p-p and Pb-Pb collisions. This behavior is naturally explained by the clustering of color sources. The change in the behavior of n is related to the formation of a large cluster of the initial color sources (partons), which marks the percolation phase transition.

The cluster-size distribution is a Γ distribution that is also the stationary solution of the Fokker-Planck equation associated with the Langevin equation for a white stochastic Gaussian noise.

Also, we have shown that the multiplicity parton distribution for events with at least one hard parton is the Γ distribution. Using this result, we compute the von Neumann entanglement entropy. In agreement with previous results, the leading term is the logarithm of the number of partons, meaning that the n microstates are equally probable and the entropy is maximal. The corrections to the leading term depend on the inverse of the normalized multiplicity parton fluctuations. At present energies available at the LHC, they are not very large for p-p and Pb-Pb collisions, however, asymptotically, they change the entanglement entropy from $\ln n$ to $\ln \sqrt{n}$. We show that in the clustering of color sources the difference between the entanglement entropy and the leading term, $S^c - \ln n$, as a function of the energy or centrality, presents a maximum corresponding to a critical density of the strings formed in the collision, the string percolation, which occurs when the overlapping strings cross all the collision surface.

ACKNOWLEDGMENTS

We are grateful for a grant from the María de Maeztu Unit of Excellence of Spain and the support of Xunta de Galicia under Project No. ED431C2017. This work has been partially carried out under Project No. FPA2017-83814-P of Ministerio de Ciencia, Innovación y Universidades (Spain).

[1] O. K. Baker and D. E. Kharzeev, Thermal radiation and entanglement in proton-proton collisions at the LHC, Phys. Rev. D **98**, 054007 (2018).
[2] D. E. Kharzeev and E. M. Levin, Deep inelastic scattering as a probe of entanglement, Phys. Rev. D **95**, 114008 (2017).
[3] J. Bergers, S. Floerchinger, and R. Venugopalan, Dynamics of entanglement in expanding quantum fields, J. High Energy Phys. 04 (2018) 145.
[4] J. Bergers, S. Floerchinger, and R. Venugopalan, Thermal excitation spectrum from entanglement in an expanding quantum string, Phys. Lett. B **778**, 442 (2018).
[5] D. E. Kharzeev and K. Tuchin, From color glass condensate to quark gluon plasma through the event horizon, Nucl. Phys. A **753**, 316 (2005).
[6] A. Bialas, Fluctuations of string tension and transverse mass distribution, Phys. Lett. B **466**, 301 (1999).
[7] J. Dias de Deus and C. Pajares, Percolation of color sources and critical temperature, Phys. Lett. B **642**, 455 (2006).
[8] P. Castorina, D. Kharzeev, and H. Satz, Thermal hadronization and Hawking-Unruh radiation in QCD, Eur. Phys. J. C **52**, 187 (2007).
[9] D. E. Kharzeev, E. Levin, and K. Tuchin, Multiparticle production and thermalization in high-energy QCD, Phys. Rev. C **75**, 044903 (2007).
[10] A. A. Bylinkin and A. A. Rostovtsev, Role of quarks in hadroproduction in high energy collisions, Nucl. Phys. B **888**, 65 (2014).
[11] A. A. Bylinkin, M. G. Ryskin, and A. A. Rostovtsev, Charged hadron distributions in a two component model, Nucl. Part. Phys. Proc. **273-275**, 2746 (2016).
[12] A. A. Bylinkin, D. E. Kharzeev, and A. A. Rostovtsev, The origin of thermal component in the transverse momentum spectra in high energy hadronic processes, Int. J. Mod. Phys. E **23**, 1450083 (2014).
[13] ALICE Collaboration, Enhanced production of multi-strange hadrons in high-multiplicity proton-proton collisions, Nat. Phys. **13**, 535 (2017).
[14] ALICE Collaboration, Multiplicity dependence of the average transverse momentum in pp, p-Pb, and Pb-Pb collisions at the LHC, Phys. Lett. B **727**, 371 (2013).
[15] M. A. Braun *et al.*, De-confinement and clustering of color sources in nuclear collisions, Phys. Rep. **599**, 1 (2015).
[16] N. Armesto, M. A. Braun, E. G. Ferreiro, and C. Pajares, Percolation Approach to Quark-Gluon Plasma and J/Ψ Suppression, Phys. Rev. Lett. **77**, 3736 (1996).
[17] M. Nardi and H. Satz, String clustering and J/Ψ suppression in nuclear collisions, Phys. Lett. B **442**, 14 (1998).
[18] J. Dias de Deus, E. G. Ferreiro, C. Pajares, and R. Ugoccioni, Universality of the transverse momentum distributions in the framework of percolation of strings, Eur. Phys. J. C **40**, 229 (2005).
[19] J. Dias de Deus, E. G. Ferreiro, C. Pajares, and R. Ugoccioni, Schwinger model and string percolation in hadron-hadron and heavy ion collisions, Phys. Lett. B **581**, 156 (2004).
[20] M. A. Braun and C. Pajares, Implication of percolation of color strings on multiplicities, correlations and the transverse momentum, Eur. Phys. J. C **16**, 349 (2000).
[21] M. A. Braun and C. Pajares, Transverse Momentum Distributions and Their Forward-Backward Correlations in the Percolating Color String Approach, Phys. Rev. Lett. **85**, 4864 (2000).
[22] G. Wilk and Z. Wlodarczyk, Interpretation of the Nonextensivity Parameter q in Some Applications of Tsallis Statistics and Lévy Distributions, Phys. Rev. Lett. **84**, 2770 (2000).
[23] T. S. Biro and A. Jakovac, Power-Law Tails from Multiplicative Noise, Phys. Rev. Lett. **94**, 132302 (2005).
[24] C. Andres, A. Moscoso, and C. Pajares, Universal geometrical scaling for hadronic interactions, Nucl. Phys. A **901**, 14 (2013).

[25] J. Dias de Deus, C. Pajares, and C. A. Salgado, Moment analysis, multiplicity distributions and correlations in high energy processes: Nucleus-nucleus collisions, Phys. Lett. B **407**, 335 (1997).

[26] J. Dias de Deus, C. Pajares, and C. A. Salgado, Production associated to rare events in high energy hadron-hadron collisions, Phys. Lett. B **408**, 417 (1997).

[27] J. Dias de Deus, C. Pajares, and C. A. Salgado, Multiplicity and transverse energy distributions associated to rare events in nucleus-nucleus collisions, Phys. Lett. B **409**, 474 (1997).

[28] J. Dias de Deus, C. Pajares, and C. A. Salgado, Rare event triggers in hadronic and nuclear collisions, Phys. Lett. B **442**, 395 (1998).

[29] M. A. Braun and C. Pajares, Self-similarity of multiplicity distributions and the KNO scaling, Phys. Lett. B **444**, 435 (1998).

[30] R. Blankenbecler *et al.*, Unusual shadowing effects in particle production off nuclei, Phys. Lett. B **107**, 106 (1981).

[31] C. Pajares and A. V. Ramallo, Parton model description of annihilations on nuclei, Phys. Lett. B **107**, 373 (1981).

[32] G. Jona-Lasinio, The renormalization group: A probabilistic view, Nuovo Cimento B **26**, 99 (1975).

[33] A. Deppman, T. Frederico E. Megias, and D. P. Menezes, Fractal structure and nonextensive statistics, Entropy **20**, 633 (2018).

[34] J. Dias de Deus and C. Pajares, String percolation and the glasma, Phys. Lett. B **695**, 211 (2011).